RSC Advances

This is an *Accepted Manuscript*, which has been through the Royal Society of Chemistry peer review process and has been accepted for publication.

Accepted Manuscripts are published online shortly after acceptance, before technical editing, formatting and proof reading. Using this free service, authors can make their results available to the community, in citable form, before we publish the edited article. This *Accepted Manuscript* will be replaced by the edited, formatted and paginated article as soon as this is available.

You can find more information about *Accepted Manuscripts* in the Information for Authors.

Please note that technical editing may introduce minor changes to the text and/or graphics, which may alter content. The journal's standard Terms & Conditions and the Ethical guidelines still apply. In no event shall the Royal Society of Chemistry be held responsible for any errors or omissions in this *Accepted Manuscript* or any consequences arising from the use of any information it contains.

ROYAL SOCIETY OF CHEMISTRY

www.rsc.org/advances

RSC Advances

RSCPublishing

ARTICLE

Rational Design of Triazatruxene-based Hole Conductors for Perovskite Solar Cells

Cite this: DOI: 10.1039/xoxxoooooox

F. Javier Ramos[a], Kasparas Rakstys[b,c], Samrana Kazim[a], Michael Grätzel[b], Mohammad Khaja Nazeeruddin[c] and Shahzada Ahmad[a*]

Received ooth January 2012,
Accepted ooth January 2012

DOI: 10.1039/xoxxoooooox

www.rsc.org/

Triazatruxene core based hole transporting materials (HTMs), **HMDI** (5,10,15-trihexyl-3,8,13-trimethoxy-10,15-dihydro-5H-diindolo[3,2-a:3',2'-c]carbazole) and **HPDI** (5,10,15-tris(4-(hexyloxy)phenyl)-10,15-dihydro-5H-diindolo[3,2-a:3',2'-c]carbazole) were synthesized and exploited in perovskite based solar cells. The energy levels of star-shaped **HMDI** and **HPDI** were tuned by symmetrically introducing electron-rich alkoxy side groups. These soluble and easily synthesized materials exhibit optical transparency in visible region, high thermal stability and have suitable HOMO values with respect to perovskite, making them an ideal HTM candidate for efficient perovskite solar cells. The **HPDI** molecule-based devices gave competitive power conversion efficiencies of ~ 11% under AM 1.5G illumination. The facile synthetic approach using inexpensive precursor materials will facilitate triazatruxene-based molecules to be further exploited in thin film organic-inorganic perovskite solar cells and needs optimization to enhance power conversion efficiency.

Introduction

Hybrid organic-inorganic perovskite, a mineral has now emerged as wonder material and is being used as semiconducting pigment for thin film solar cells fabrication.[1,2] The recent surge of interest in perovskite based solar cells further encouraged scientist and technologist across the world to study it further[3–13] and now it is clear that perovskite solar cells are no more just lab curiosity. Perovskite is being probed as semiconducting pigment due to its excellent absorption in visible light,[14,15] high charge carrier mobility (both electrons and holes) and long carrier diffusion length.[14,16–18] Competitive light to energy conversion efficiencies have been obtained in labs, which are very close to established thin film solar cells and is being viewed as viable technology in photovoltaic category.[19] The devices, prepared using mesoporous photoanode as an electron acceptor (hole blocking layer), perovskite as light harvester, hole transport materials (HTM) as a hole extraction layer (electron blocking layer) and gold as a contact (cathode) have gained significant interest due to the ease of fabrication, flexibility in the selection of materials and cost effective production. Moreover reproducible results across the labs were obtained, which states its suitability. Currently, in most of the high performing devices *Spiro*-OMeTAD (2,2',7,7'-tetrakis(*N*,*N*-di-*p*-methoxyphenylamine)-9,9-spirobifluorene) is being used to transport holes from the working electrode. In the recent past, sincere attempts were made to find an alternate organic HTM to rival the use of *Spiro*-OMeTAD. In some cases, poor matching of highest occupied molecular orbital (HOMO) level and incomplete pore filling by the perovskites induce hindrance in its successful application. The ideal HTM should have sufficient hole mobility, thermal and UV stability, and suitable HOMO energy level. Some *p*-type polymer poly[*N*-9-heptadecanyl-2,7-carbazole-alt-3,6-bis-(thiophen-5-yl)-2,5-dioctyl-2,5-dihydropyrrolo[3,4]pyrrole-1,4-dione] (PCBTDPP) was used in $CH_3NH_3PbBr_3$ perovskites based cells and gave relatively low PCE of 3%[20], while this PCE reached to 5.55% in the case of $CH_3NH_3PbI_3$ and due to its better absorption[21]. Other polymer based HTM such as P3HT,[21,22] poly-[2,1,3-benzothiadiazole-4,7-diyl[4,4-bis(2-ethylhexyl)-4*H*-cyclopenta[2,1-*b*:3,4*b*]dithiophene-2,6-diyl]] (PCPDTBT),[21] poly-[[9-(1-octylnonyl)-9*H*-carbazole-2,7-diyl]-2,5-thiophenediyl-2,1,3-benzothiadiazole-4,7-diyl-2,5-thiophenediyl] (PCDTBT),[21] and poly(triarylamine) (PTAA) were also used.[19,21] Among the recent reports of using different *p*-type polymers, only PTAA showed remarkable PV behavior. The polymeric nature induces large chains, which will lead to defects and improper intimate contact with layers where the polymer is in between and eventually results in poor reproducibility. Additionally polymers are known to be unstable in the low vacuum conditions making difficult deposition of the metallic contact on the top. Some new approaches, like p-type polymer composites with carbon nanotubes (P3HT/SWNTs)[23] were able to perform well in

RSC Advances Accepted Manuscript

terms of efficiency (15.3%). Contrary to the polymers, inorganic compounds like CuI[24] (PCE=6%) and small organic molecules with having different nature were also reported as HTMs. Among them promising efficiencies with Zn phtalocyanine based: TT80[25] (6.7%), diacetylide triphenilamine based: MeODATPA[26] (8.8%), carbazole based: X51[27] (9.8%) and SGT405[28] (14.8%), tetrathiafulvalene based: TTF-1[29] (11.03%), pyrene based: Py-C[30] (12.4%), quinolizino acridine based: Fused-F[31] (12.8%), 3,4-ethylenedioxythiophene based: H101[32](13.8%), TIPS-pentacene (11.8%)[32] and Spiro-OMeTAD derivatives[33] (16.7%). These small organic molecules presented less important problems of reproducibility, stability and resulted in better contact between absorber and metal contact than their *p*-type polymeric counterparts.

Triazatruxene-based HTM were earlier used in organic solar cells[34]. Those molecules consist of a core, made of three indole units combined by one benzene ring. The presence of benzene ring provides an extended delocalized π-system, providing excellent electron-donating potential for intramolecular charge transfer. Additionally, it permits to tune their electronic and optical properties. However, the reported compounds were not soluble, thus limiting their deposition techniques to evaporation routes, which are cost uneffective due to the requirement of huge equipments and vacuum system. Here we report facile synthesis and characterization of two soluble, planar triazatruxene core based HTMs (5,10,15-trihexyl-3,8,13-trimethoxy-10,15-dihydro-5*H*-diindolo[3,2-*a*:3',2'-*c*]carbazole **HMDI** and 5,10,15-tris(4-(hexyloxy)phenyl)-10,15-dihydro-5*H*-diindolo[3,2-*a*:3',2'-*c*]carbazole **HPDI** and their exploitation in perovskite solar cells. The energy levels of **HMDI** (-5.17) and **HPDI** (-5.41eV) were tuned according to the perovskite energy levels by simple introduction of electron-donating methoxy- and (*p*-hexyloxy)phenyl-side groups on the triazatruxene core. They are easily synthesized, soluble materials, have good optical transparency in visible region, and shows high thermal stability.

Results and discussion

Fig. 1 illustrates chemical structures of **HMDI** and **HPDI** and a scheme 1 shows the synthetic routes used from triazatruxene as starting molecule. The experimental details and the adopted synthesis route are explained in the experimental section. Both molecules are highly soluble in a variety of non-polar solvents and thus, enjoy the privilege to be solution processed. The high solubility and choice of solvents such as chlorobenzene or toluene, due to the presence of hexyl chains offers its application for variety of devices including organic solar cells, solid state dye-sensitized and perovskite solar cells. **HMDI** and **HPDI** presented solubility at room temperature >100 mg·mL^{-1}, both in chlorobenzene and toluene, thus making possible facile and cost effective solution processed deposition techniques as spin-coating, dip-coating or drop-casting.

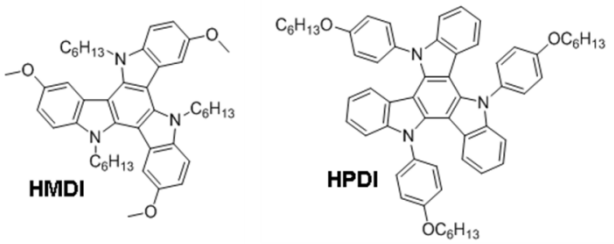

Figure 1. Chemical structures of HMDI and HPDI hole transporting materials

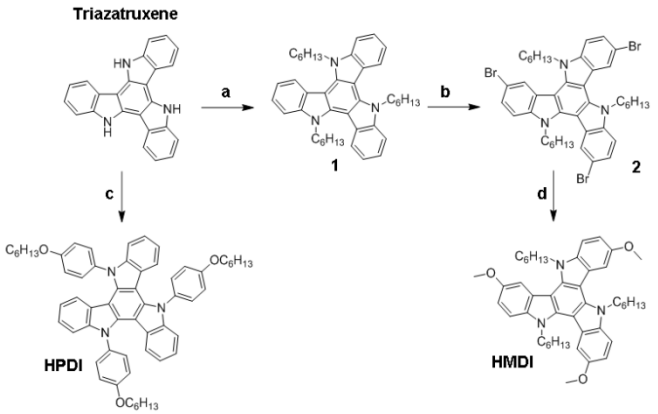

Scheme 1. Synthetic route for the HMDI and HPDI HTMs. More details in the Supporting Information.

The presence of alkoxy groups (methoxy for **HMDI** and (*p*-hexyloxy) phenyl in the case of **HPDI**) allows tuning the HOMO level in order to adapt the molecule's donor nature. Furthermore, alkoxy groups have been demonstrated in literature as effective anchors for the interface between perovskite/HTM[35]. The UV-visible absorbance spectra of **HMDI** and **HPDI** solution in chlorobenzene are shown in Fig. 2a. Both molecules absorb in the range of 300-400 nm. The absorption spectra shows broad absorption band at peak maximum around 317 and 325 nm, which arises due to π-π* transition.

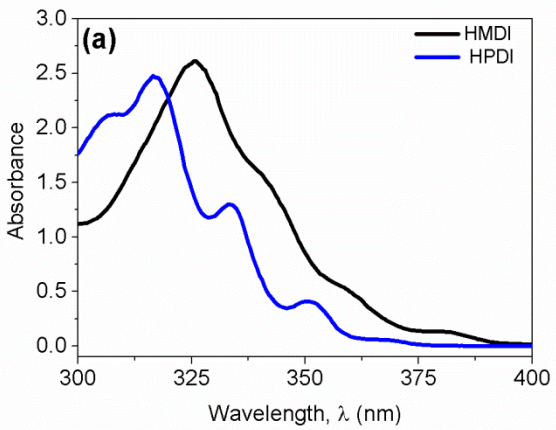

RSC Advances Accepted Manuscript

This journal is © The Royal Society of Chemistry 2012

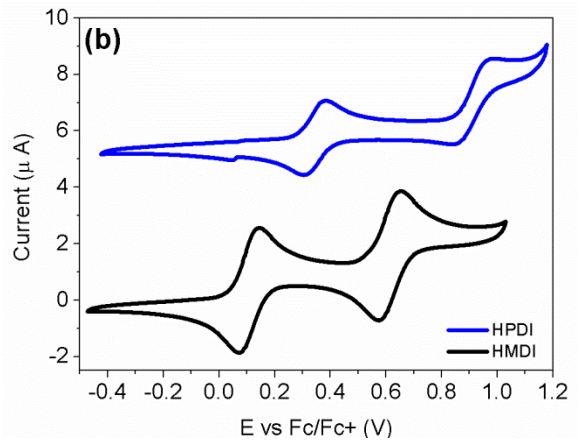

Fig. 2. a) UV-Vis absorbance spectra of HTMs measured in diluted solution of chlorobenzene and b) cyclic voltammograms of HTMs measured in 0.1 M solution of Tetra-n-butylammonium hexafluorophosphate in dichloromethane solvent using glassy carbon working electrode, Pt reference electrode, and Pt counter electrode with Fc/Fc^{+} as an internal standard. To match the scale the current on Y-axis was offset to 5.5 μA in case of HPDI curve.

The UV-Vis absorbance and cyclic voltammetry measurements of these HTMs (Fig. 2b) were used to study the HOMO/LUMO energy levels and band gap. In CV graph, both HTMs shows reversible redox peak showing good electrochemical stability. The corresponding data are given in Table 1. The calculated optical band gap (E_g) from the onset of absorption band was at 3.14eV and 3.26eV for **HMDI** and **HPDI**, respectively. HOMO levels of **HMDI** (-5.17eV) and **HPDI** (-5.41eV) are well aligned with the perovskite valence band (-5.44eV).

Table 1. Summary of optical, electrochemical and thermal properties for the studied HTMs.

Compound	λ_{onset} (nm)[a]	E_g opt (eV)[b]	HOMO (eV)[c]	LUMO (eV)[d]	T_g (ºC)[e]
HMDI	395	3.14	-5.17	-2.03	1
HPDI	380	3.26	-5.41	-2.15	36

[a]Absorption spectra were measured in DCM solution. [b] Optical Band gap (E_g) was derived from the onset of absorption. [c] The E_{HOMO} was calculated by using the equation: E_{HOMO}=-($E_{1/2}$ *vs* Fc+/Fc] +5.064)(eV), where $E_{1/2,}$ formal potential was calculated by averaging anodic peak potential and cathodic peak potential, $E_{1/2}$= (E_{pa}+E_{pc}). [d] E_{LUMO} = E_{HOMO} + E_g opt. [e]T_g = glass transition temperature calculated from DSC.

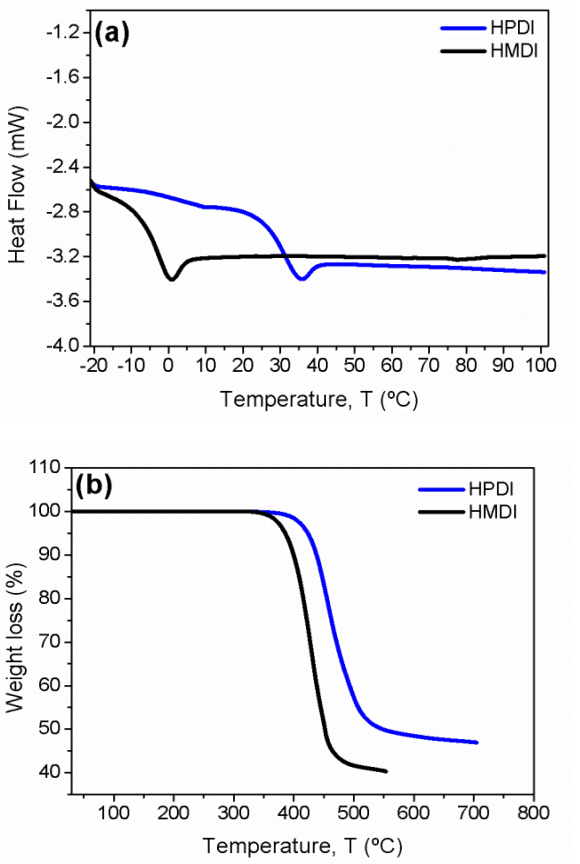

Fig. 3. Thermal characterization of triazatruxene-based HTMs, HMDI (black) and HPDI (blue). a) Differential Scanning Calorimetry (DSC) was performed at scan rate 10 $^{o}K{\cdot}min^{-1}$ in nitrogen atmosphere, and data from second cycle are presented , b) Thermogravimetric analysis (TGA) of HMDI and HPDI with scan rate of 10 $^{o}K{\cdot}min^{-1}$.

The thermal properties of novel synthesized HTMs were studied using differential scanning calorimetry (DSC) and thermogravimetric analysis (TGA) measurements (Fig. 3). Both compounds show amorphous nature, a low glass transition temperature (T_g = 1ºC for **HMDI**, T_g = 36 ºC for **HPDI**) as determined by DSC (Fig. 3a). Ideally this is an essential requirement for the intimate contact between interfaces to ensure an efficient hole extraction.[36] **HMDI** and **HPDI** are stable up to 350°C and 400°C respectively (Fig. 3b), confirming their good thermal stability and stating practical utilization.

An energy level diagram of the materials is shown in Fig. 4a, while the corresponding perovskite device configuration employing triazatruxene-based HTM is presented in Fig. 4b.

RSC Advances Accepted Manuscript

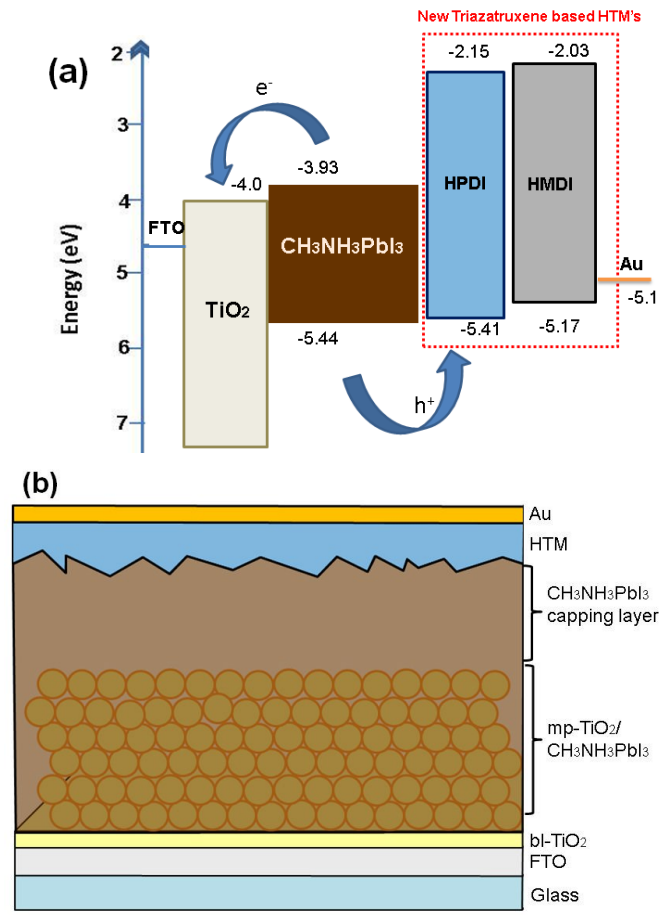

Fig. 4. a) Energy level diagram for the fabricated photovoltaic devices using **HMDI** and **HPDI** as HTMs. b) Perovskite Solar Cell architecture used for device fabrication.

To confirm the device architecture, cross sectional scanning electron microscopy (SEM) measurements were carried out (Fig. 5). Mesoporous titania can be clearly observed, with $CH_3NH_3PbI_3$ absorber both infiltrated and forming large crystals on the top of the mesoporous photoanode creating rough surface on the top of the titania. This was further smoothened by the HTM layer which has thickness of 150nm, approximately.

To study the real utilization of synthesized HTM, i.e. the photovoltaic properties, i.e. current-voltage curves were recorded for the fabricated device. **HMDI** and **HPDI** were tested as hole transporting layer and the results are presented in Table 2. The devices gave very competitive PCE and the *J-V* curves are shown in Fig. 6a. When **HMDI** was used as HTM in its pristine form (as such), an average PCE of 7.13% was measured, while for the champion cell the PCE value reached to 8.62%. The unexpectedly high open circuit voltage (V_{OC} = 907 mV - 938 mV) was obtained due to its well band alignment with the perovskite valence band.

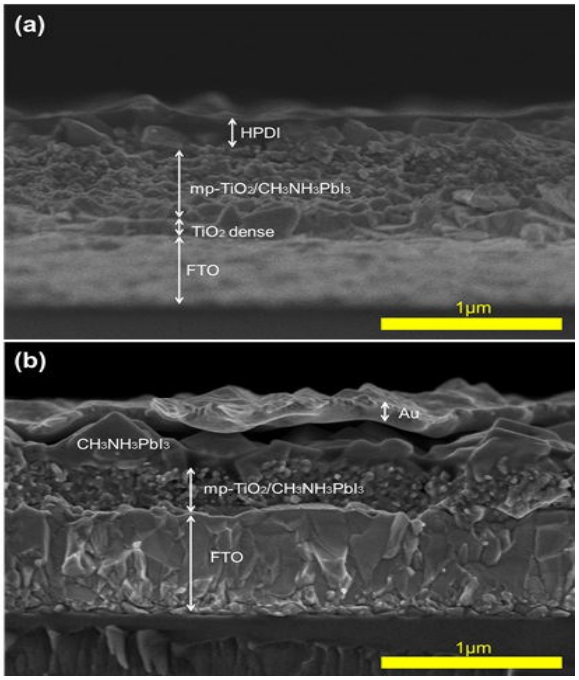

Fig. 5. (a) and (b) shows cross sectional scanning electron microscopy image of the photovoltaic devices using HPDI as HTM.

However, relatively low J_{SC} (~14mA cm^{-2}) and fill factor (FF = 0.55-0.64) were obtained. In order to improve the PV properties the conventional strategy of, doping was made and the additives such as LiTFSI and *tert*-butylpyridine (*t*-BP) were added for **HMDI**. Contrary to report for other HTM, both V_{OC} and J_{SC} were reduced after doping, pointing towards doping is not very effective in this case and possibly hindering its mobility. After doping, fill factor has significantly increased, but it can be attributed to the lower J_{SC}. The devices fabricated with pristine **HPDI**, showed improved value of PCE (Average = 9.62%). The obtained enhanced PCE was due to higher fill factors and current (J_{SC} = 16.80mA cm^{-2}, FF = 0.642), while the champion devices showed the PCE of 9.83% (J_{SC} = 16.51mA cm^{-2}, V_{OC} = 897mV, FF = 0.663). Here it should be noted that in its pristine form both the molecules performed well and showed higher PCE compare to the standard Spiro-OMeTAD. Similarly the addition of LiTFSI and *t*-BP in **HPDI** resulted in slightly improved V_{OC} and fill factor, but the short circuit current drops dramatically from 17mA cm^{-2} to less than 10 mA cm^{-2}. Thus the doping of synthesized HTM in both cases was found to be uneffective, while in the case of Spiro-OMeTAD, other organic small molecules and PTAA, doping is crucial in order to achieve high efficiency. The drop in the current might be attributed to some undesirable molecular packing between *t*-BP and HTM, introduction of trap sites, which resulted in bad interface between perovskite and HTM, particularly in the case for **HPDI**.

Further to improve the PV properties and the interface of HTM with perovskites, a nonpolar solvent such as toluene was used. Only, LiTFSI was added to increase the conductivity and the device PV was improved. Both the photocurrent and FF has

RSC Advances Accepted Manuscript

This journal is © The Royal Society of Chemistry 2012

improved significantly, and a promising PCE of 10.82% was obtained (J_{SC} = 19.16mA cm^{-2}, V_{OC} = 976mV, FF = 0.576). It is well known, that *t*-BP has a positive effect in increasing the voltage of the devices, but it also increases the recombination of electron and holes in the devices, thus making the devices less stable. Here it is notable that the devices fabricated without t-BP are working efficiently and the best results were obtained with using only 10mg/ml of HPDI while in the case of Spiro-OMeTAD, much higher amount is used (72.3mg/ml), thus making it further cost-effective. The devices fabricated with **HPDI** also showed good reproducibility, having low standard deviations. In order to have real figure of merit the devices were measure from V_{oc}→J_{sc} at voltage sweep rate of 0.1V/sec, proper mask size was also utilized us to avoid any pronounce hysteresis effect. Fig.S1 shows the hysteresis curves for different HTM used for the fabrication of typical cells (not for the champion device). The incident photon to current efficiency (IPCE) spectra for the devices was shown in Fig. 6b, where the integral photocurrent obtained from the IPCE spectra are in good agreement with the experimentally obtained J_{sc} from current-voltage performance (Fig. S2). The doped **HPDI** showed improved light harvesting abilities than their analogous family members and in the visible range it approaches 90% conversion rate.

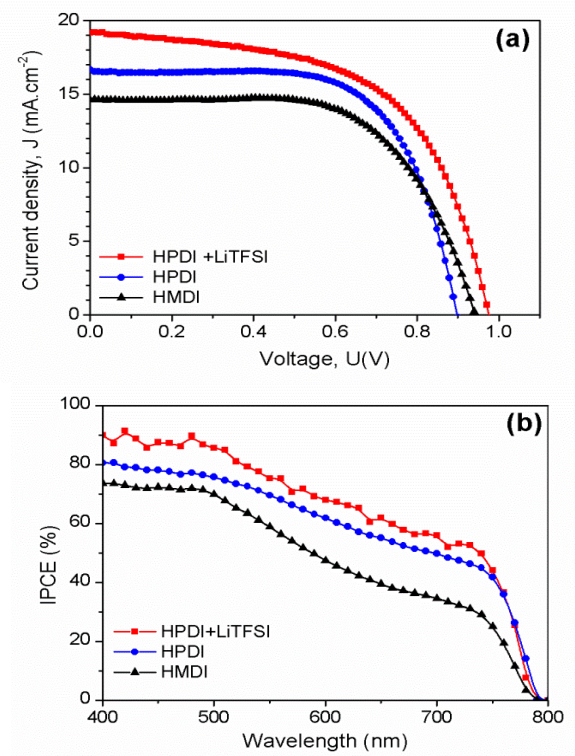

Fig. 6. a) Current-Voltage characteristics for the perovskite solar cells employing HPDI with LiTFSI salt as additive (red), pristine HPDI (blue) and pristine HMDI (black), b) IPCE spectra for the devices shown in Fig. 6a.

Table 2. Photovoltaics parameters derived from *J-V* measurements for $CH_3NH_3PbI_3$ perovskite based solar cells using the synthesized triazatruxene molecules.[a]

HTM		J_{SC} (mA cm^{-2})	V_{OC} (V)	Fill Factor	*PCE* (%)
HMDI		14.43	0.938	0.637	8.62
	Avg.± SD	14.31±1.73	0.907±0.03	0.551±0.07	7.13±1.14
HPDI		16.51	0.897	0.663	9.83
	Avg.± SD	16.80±0.23	0.893±0.01	0.642±0.02	9.62±0.17
HPDI+LiTFSI[b]		19.16	0.976	0.576	10.82
	Avg.± SD	18.69±0.39	0.961±0.02	0.562±0.01	10.15±0.53
Spiro-OMeTAD[b]		19.62	944.137	0.694	12.93

[a]Average data and standard deviation calculated for 3 individual cells in the same batch. Mask size: 0.16cm^2 though the active area was ~0.6cm^2.
[b]Measured at 99.5mW·cm^{-2} under AM 1.5G spectra.

Experimental Section

a) 5,10,15-tris(4-(hexyloxy)phenyl)-10,15-dihydro-5H-diindolo[3,2-a:3',2'-c]carbazole (**HPDI**).
To a solution of triazatruxene (250 mg, 0.74 mmol, 1 eq.), 1-(hexyloxy)-4-iodobenzene[37] (0.9 g, 3 mmol, 4 eq.) in 5 mL of quinoline, CuI (550 mg, 2.9 mmol, 4 eq.) and K_2CO_3 (400 mg, 2.9 mmol, 4 eq.) were added. After stirring at 190 °C overnight under a N_2 atmosphere, the reaction mixture was allowed to cool to room temperature and subsequently diluted with DCM followed by filtering through a plug of celite. The filtrate was concentrated in a vacuum. The residue was purified by column chromatography eluting with 30 % DCM in hexane to give 170 mg of pale yellow solid (55 %). ^{1}H NMR (400 MHz, $CDCl_3$-d) δ 7.59 (d, J = 6.8 Hz, 6H), 7.30 (d, J = 8.3 Hz, 6H), 7.13 – 7.25 (m, 6H), 6.85 (t, J = 8.0 Hz, 3H), 6.21 (d, J = 8.1 Hz, 3H), 4.14 (t, J = 5.9 Hz, 6H), 2.13 – 1.83 (m, 6H), 1.44 (t, J = 57.8 Hz, 18H), 0.98 (s, 9H). ^{13}C NMR (100 MHz, C_6D_6-d_6) δ 159.06, 142.55, 138.43, 133.86, 130.08, 127.57, 123.18, 123.07, 120.23, 115.53, 110.28, 104.58, 68.04, 31.58, 29.15, 25.72, 22.67, 13.94. $C_{60}H_{63}N_3O_3[M^+]$ Exact Mass = 873.4869, MS (MALDI-TOF) = 873.1144.

b) 5,10,15-trihexyl-3,8,13-trimethoxy-10,15-dihydro-5H-diindolo[3,2-a:3',2'-c]carbazole (**HMDI**).
In a 50 mL three-necked flask, a solution of 1.95 mL (10.5 mmol, 15 eq.) of sodium methoxide 5.4 M in methanol, dry DMF (15 mL), copper(I) iodide (810 mg, 4.3 mmol, 6 eq.), 3,8,13-tribromo-5,10,15-trihexyl-10,15-dihydro-5H-diindolo[3,2-a:3',2'-c]carbazole (0.6 g, 0.72 mmol, 1 eq.) was heated to reflux for 3 h under a N_2 atmosphere. After that, solution was filtered while hot through the celite to remove copper(I) iodide and washed with water. The mixture was extracted with DCM and organic phase was dried over $MgSO_4$. The product was isolated off on a silica gel column with 50 % DCM in hexane to give a product as a pale yellow solid (300 mg, 55 %). ^{1}H NMR (400 MHz, $CDCl_3$-d) δ 8.05 (d, J = 8.0 Hz,

RSC Advances Accepted Manuscript

3H), 7.71 (s, 3H), 7.55 (d, J = 8.0 Hz, 3H), 4.95 (s, 6H), 4.03 (s, 9H), 2.02 (m, 6H), 1.41 – 1.28 (m, 18H), 0.84 (t, J = 7.0 Hz, 9H). ^{13}C NMR (100 MHz, Benzene-d_6) δ 157.31, 143.12, 138.04, 122.55, 118.14, 107.27, 104.20, 95.97, 55.02, 46.71, 31.23, 29.28, 26.23, 22.35, 13.71. $C_{45}H_{57}N_3O_3[M^+]$ Exact Mass = 687.44, MS (ESI) = 687.46.

Device fabrication

FTO-coated glass (NSG10) was laser etched, cleaned with Hellmanex and rinsed with deionized water and ethanol. Then the electrodes were ultrasonicated in 2-propanol and dried with compressed air. The substrates were UV/O_3 treated to eliminate organic residues before blocking layer depositon.

A blocking TiO_2 layer was deposited by spray pyrolysis using a titanium diisopropoxide bis(acetyl acetonate) solution (1mL of commercial titanium diisopropoxide bis(acetyl acetonate) 75% in 2-propanol was diluted with 19mL of absolute ethanol) using O_2 as carrier gas. During this process, etched substrates were heated at 450 ºC to help the anatase formation. After cooling down, substrates were immersed in $TiCl_4$ 20mM aqueous solution and baked 30 minutes at 70ºC. Then the samples were washed with deionized water and heated 500ºC for 30 minutes. TiO_2 mesoporous layer (mp-TiO_2) was prepared by spin coating 35µL per cell of a solution made of 1g of 30NR-D in 3.5g of absolute ethanol. The spin coating conditions employed were: speed=4000rpm, acceleration=2000rpm·s^{-1}, time=30s. Subsequently, samples were sequentially sintered: 125ºC for 5min, 325ºC for 5min, 375ºC for 5min, 450ºC for 15min and 500ºC for 15min.

A PbI_2 solution 1.25M concentrated in DMF was kept at 70ºC to avoid any precipitation. 50µL from that solution were deposited and spun coated over the mesoporous TiO_2 film (speed=6500rpm, acceleration=5500rpm·s^{-1}, time=30s). Immediately, the films (electrodes) were annealed at 70ºC for 30 minutes. After cooling down, the spin coating process was repeated using the same spin-coating parameters. 100 µL of CH_3NH_3I solution (8mg·mL^{-1}) were spread above the PbI_2 film to form perovskite, the waiting time was 20-25s to observe the conversion of PbI_2 into $CH_3NH_3PbI_3$ (from yellow to black). Followed this, the excess of solution was removed by spin coating (speed=4000rpm, acceleration=1650rpm·s^{-1}, time=30s) and then the samples were annealed at 70ºC during 30 minutes.

Hole transporting materials (HTMs): 5,10,15-trihexyl-3,8,13-trimethoxy-10,15-dihydro-5*H*-diindolo[3,2-*a*:3',2'-*c*]carbazole (**HMDI**) and 5,10,15-tris(4-(hexyloxy)phenyl)-10,15-dihydro-5*H*-diindolo[3,2-*a*:3',2'-*c*]carbazole (**HPDI**) were both deposited by spin coating (speed=2000rpm, acceleration=1000rpm·s^{-1}, time=30s). HMDI and HPDI solutions were prepared by dissolving 30mg in 1mL of either chlorobenzene or toluene. Diluted solution were also prepared in the case of HPDI, employing LiTFSI salt as additive, for this 10mg of product was dissolved in 1mL of toluene and Li salt was added from a stock solution (170mg of LiTFSI in 1mL of acetonitrile), obtaining a molar ratio LiTFSI/HPDI=0.324 in the final solution. Finally to finish the device, a cathode of 80nm gold was thermally evaporated.

Lead iodide, methyl ammonium iodide and Spiro-OMeTAD solutions were prepared inside an argon glove box with moisture and oxygen controlled conditions. PbI_2 spin coating, MAI deposition and HTM spin coating depositions were developed inside a nitrogen dry box.

Conclusions

In summary, we have rationally designed solution-processable triazatruxene-based HTMs, and demonstrated their application in perovskite solar cells. These materials were synthesized using inexpensive precursors and state forward few synthetic steps compared to the expensive Spiro-OMeTAD. **HMDI** and **HPDI** have good thermal stability and are highly soluble in a variety of nonpolar solvents. The HOMO-LUMO energy levels of **HMDI** and **HPDI**, -5.17/-2.03 eV and -5.41/-2.15 eV, respectively, are well aligned with respect to perovskite energy level. **HMDI** and **HPDI** showed 8.6% and 9.8% PCE without the use of any additive, which is higher than reported for Spiro-OMeTAD. In the case of **HPDI,** the light to electricity conversion efficiency was improved to 10.82% with the addition of only LiTFSI salt, due to significantly enhancement in J_{SC} and V_{OC}. We believe that triazatruxene core-based HTMs have potential to be an alternative for expensive Spiro-OMeTAD and *p*-type polymers in hole transporting layers due to their ease of fabrication, potentially low price, excellent solubility and remarkable thermal properties.

Conflict of interest

Authors from Abengoa Research may have competing interests as Abengoa is an international company and has significant interest in the renewable energy sector. Patent disclosing the work is pending.

Acknowledgements

Notes and references

[a] Abengoa Research, Abengoa, Campus Palmas Altas-41014, Seville, Spain. Email: shahzada.ahmad@abengoa.com
[b] Laboratory of Photonics and Interfaces, Department of Chemistry and Chemical Engineering, École Polytechnique Fédérale de Lausanne, Station 6, CH-1015, Lausanne, Switzerland.
[c]Group for Molecular Engineering of Functional Materials, Institute of Chemical Sciences and Engineering, École Polytechnique Fédérale de Lausanne, CH-1015-Lausanne, Switzerland

Electronic Supplementary Information (ESI) available: Experimental details: materials, synthesis, and characterization. IPCE with integrated photocurrent is also included. See DOI: 10.1039/b000000x/

1 S. Kazim, M. K. Nazeeruddin, M. Grätzel, and S. Ahmad, *Angew. Chem. Int. Ed. Engl.*, 2014, **53**, 2812–24; *Angewandte Chemie*, 2014, **126**, 2854–2867
2 I. Chung, B. Lee, J. He, R. P. H. Chang, and M. G. Kanatzidis, *Nature*, 2012, **485**, 486–9.
3 A. Kojima, K. Teshima, Y. Shirai, and T. Miyasaka, *J. Am. Chem. Soc.*, 2009, **131**, 6050–6051.

RSC Advances Accepted Manuscript

 This journal is © The Royal Society of Chemistry 2012

4 H.-S. Kim, C.-R. Lee, J.-H. Im, K.-B. Lee, T. Moehl, A. Marchioro, S.-J. Moon, R. Humphry-Baker, J.-H. Yum, J. E. Moser, M. Grätzel, and N.-G. Park, *Sci. Rep.*, 2012, **2**, 591.
5 M. M. Lee, J. Teuscher, T. Miyasaka, T. N. Murakami, and H. J. Snaith, *Science*, 2012, **338**, 643–647.
6 J. H. Noh, S. H. Im, J. H. Heo, T. N. Mandal, and S. Il Seok, **2**, 28–31.
7 J. Burschka, N. Pellet, S.-J. Moon, R. Humphry-Baker, P. Gao, M. K. Nazeeruddin, and M. Grätzel, *Nature*, 2013, **499**, 316–9.
8 J.-H. Im, I.-H. Jang, N. Pellet, M. Grätzel, and N.-G. Park, *Nat. Nanotechnol.*, 2014, **9**, 927–932.
9 N. Pellet, P. Gao, G. Gregori, T.-Y. Yang, M. K. Nazeeruddin, J. Maier, and M. Grätzel, *Angew. Chem. Int. Ed. Engl.*, 2014, **53**, 3151–7.
10 A. Mei, X. Li, L. Liu, Z. Ku, T. Liu, Y. Rong, M. Xu, M. Hu, J. Chen, Y. Yang, M. Gratzel, and H. Han, *Science*, 2014, **345**, 295–298.
11 M. I. Dar, F. J. Ramos, Z. Xue, B. Liu, S. Ahmad, S. A. Shivashankar, M. K. Nazeeruddin, and M. Grätzel, *Chem. Mater.*, 2014, 26, 4675–4678.
12 F. J. Ramos, M. C. López-Santos, E. Guillén, M. K. Nazeeruddin, M. Grätzel, A. R. Gonzalez-Elipe, and S. Ahmad, *ChemPhysChemchem*, 2014, **15**, 1148–53; F. J. Ramos, M. Oliva-Ramirez, M. K. Nazeeruddin, M. Grätzel, A. R. Gonzalez-Elipe, and S. Ahmad, *J. Mater. Chem. A*, (2015), DOI: 10.1039/c5ta02238j.
13 F. Hao, C. C. Stoumpos, D. H. Cao, R. P. H. Chang, and M. G. Kanatzidis, *Nat. Photon.*, 2014, **8**, 489–494.
14 K. Tanaka, T. Takahashi, T. Kondo, K. Umeda, K. Ema, T. Umebayashi, K. Asai, K. Uchida, and N. Miura, *Jpn. J. Appl. Phys.*, 2005, **44**, 5923–5932.
15 C. C. Stoumpos, C. D. Malliakas, and M. G. Kanatzidis, *Inorg. Chem.*, 2013, **52**, 9019–38.
16 K. Tanaka, T. Takahashi, T. Ban, T. Kondo, K. Uchida, and N. Miura, *Solid State Commun.*, 2003, **127**, 619–623.
17 V. W. Bergmann, S. A. L. Weber, F. J. Ramos, M. K. Nazeeruddin, M. Grätzel, D. Li, A. L. Domanski, I. Lieberwirth, S. Ahmad, and R. Berger, *Nat. Commun.*, 2014, **5:5001**, 1–9.
18 E. Guillén, F. J. Ramos, J. A. Anta, and S. Ahmad, *J. Phys. Chem. C*, 2014, **118 (40)**, 22913–22922.
19 N. J. Jeon, J. H. Noh, W. S. Yang, Y. C. Kim, S. Ryu, J. Seo, and S. Il Seok, *Nature*, 2015, **517**, 476–480.
20 B. Cai, Y. Xing, Z. Yang, W.-H. Zhang, and J. Qiu, *Energy Environ. Sci.*, 2013, **6**, 1480.
21 J. H. Heo, S. H. Im, J. H. Noh, T. N. Mandal, C.-S. Lim, J. A. Chang, Y. H. Lee, H. Kim, A. Sarkar, M. K. Nazeeruddin, M. Graetzel, and S. Il Seok, *Nat. Photon.*, 2013, **7**, 486–491.
22 D. Bi, L. Yang, G. Boschloo, A. Hagfeldt, and E. M. J. Johansson, *J. Phys. Chem. Lett.*, 2013, **4**, 1532–1536.
23 S. N. Habisreutinger, T. Leijtens, G. E. Eperon, S. D. Stranks, R. J. Nicholas, and H. J. Snaith, *Nano Lett.*, 2014, **14**, 5561–5568.
24 J. A. Christians, R. C. M. Fung, and P. V Kamat, *J. Am. Chem. Soc.*, 2013, **136**, 758–764.
25 F. J. Ramos, M. Ince, M. Urbani, A. Abate, M. Grätzel, S. Ahmad, T. Torres, and N. Mohammad K., *Dalt. Trans.*, 2015, DOI:10.1039/c5dt00396b.
26 A. Abate, M. Planells, D. J. Hollman, V. Barthi, S. Chand, H. J. Snaith, and N. Robertson, *Phys. Chem. Chem. Phys.*, 2015, **17**, 2335–2338.
27 B. Xu, E. Sheibani, P. Liu, J. Zhang, H. Tian, N. Vlachopoulos, G. Boschloo, L. Kloo, A. Hagfeldt, and L. Sun, *Adv. Mater.*, 2014, **26**, 6629–6634.
28 S. Do Sung, M. S. Kang, I. T. Choi, H. M. Kim, H. Kim, M. Hong, H. K. Kim, and W. I. Lee, *Chem. commun.*, 2014, **50**, 14161–14163.
29 J. Liu, Y. Wu, C. Qin, X. Yang, T. Yasuda, A. Islam, K. Zhang, W. Peng, W. Chen, and L. Han, *Energy Environ. Sci.*, 2014, **7**, 2963–2967.
30 N. J. Jeon, J. Lee, J. H. Noh, M. K. Nazeeruddin, M. Grätzel, and S. Il Seok, *J. Am. Chem. Soc.*, 2013, **135**, 19087–90.
31 P. Qin, S. Paek, M. I. Dar, N. Pellet, J. Ko, M. Grätzel, and M. K. Nazeeruddin, *J. Am. Chem. Soc.*, 2014, **136**, 8516–9.
32 H. Li, K. Fu, A. Hagfeldt, M. Grätzel, S. G. Mhaisalkar, and A. C. Grimsdale, *Angew. Chem. Int. Ed. Engl.*, 2014, **53**, 4085–8; S. Kazim, F. J. Ramos, P. Gao, M. K. Nazeeruddin, M. Grätzel, and S. Ahmad, *Energy Environ. Sci.*, 2015, DOI: 10.1039/C5EE00599J
33 N. J. Jeon, H. G. Lee, Y. C. Kim, J. Seo, J. H. Noh, J. Lee, and S. Il Seok, *J. Am. Chem. Soc.*, 2014, **136**, 7837–40.
34 C. Kulshreshtha, G. W. Kim, R. Lampande, D. H. Huh, M. Chae, and J. H. Kwon, *J. Mater. Chem. A*, 2013, **1**, 4077.
35 A. Torres and L. G. C. Rego, *J. Phys. Chem. C*, 2014.
36 T. Leijtens, I. Ding, T. Giovenzana, J. T. Bloking, M. D. Mcgehee, and A. Sellinger, *ACS Nano*, 2012, **6**, 1455–1462.
37 Y. Arakawa, S. Nakajima, R. Ishige, M. Uchimura, S. Kang, G. Konishi, and J. Watanabe, *J. Mater. Chem.*, 2012, **22**, 8394.

RSC Advances Accepted Manuscript

TOC graphic:

Solution processable, triazatruxene based hole-transporting materials were synthesized using inexpensive precursors with state forward synthetic steps and gave good performance in perovskite based solar cells.

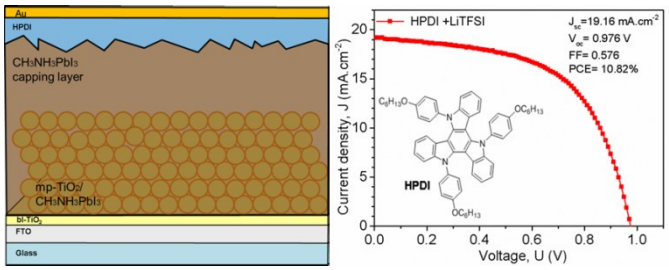

RSC Advances Accepted Manuscript

This journal is © The Royal Society of Chemistry 2012